

# Correspondence

## Analysis and Calibration of a Reflection Coefficient Bridge for Use with Any Waveguide Mode

Single-frequency measurements of both absolute phase and absolute magnitude of a complex reflection coefficient are required in determining complex permittivity by the Roberts-von Hippel [1] method. The slotted line, although traditionally the basic tool for these measurements, suffers from several disadvantages. Among them are errors caused by the perturbing influence of the probe and slot and decreased precision at short (millimeter) wavelengths and low VSWR's. Reflectometers of the Engen and Beatty [2] type and "return-loss test sets" such as used by Pomeroy [3] yield high precision at low VSWR's but measure only *magnitude* and are therefore unacceptable. Some microwave bridges measure *complex* reflection coefficient, however, thus offering an effective alternative to the slotted line.

In its simplest form, the complex reflection coefficient bridge consists of a comparator network (e.g., hybrid tee, hybrid ring, opposed directional couplers, etc.) which balances the signal reflected from the unknown impedance against that reflected from a calibrated variable (complex) reflection coefficient [4], [5]. Previously, these signals have been assumed equal at balance so that specially machined comparator networks possessing extreme symmetry have been required for accurate results. This requirement is removed in the present correspondence by analyzing the bridge mathematically and using preliminary calibration measurements to take mechanical imperfections into account. Advantages of this approach are twofold. First, it allows one to obtain accurate results using an ordinary commercial grade "magic" tee as a comparator element. Second, the present bridge is extremely versatile and can contain bends, windows, mode transducers, etc., without sacrificing accuracy. We have, for example, used such a bridge to measure the reflection coefficient of the circular TE<sub>01</sub> mode at 48 GHz [6] by merely introducing a mode transducer into the sample arm and then including it in the calibration measurements.

The price one pays for these advantages is an increase in complexity of the calculations relating bridge measurements to actual magnitude and phase of reflection coefficient. For most laboratory studies, however, this disadvantage is not particularly significant and can be overcome by the use of a simple computer program to process the data.

Consider the basic bridge network of Fig. 1. The tandem combination of a precision

(rotary-vane) attenuator and a precision short circuit constitutes a variable complex reflection coefficient standard. For simplicity, the comparator network is shown as a hybrid tee in Fig. 1 although the present analysis actually applies to any "four-port" capable of producing null at balance. The waveguide mode at port 4 need not even be the same as that at port 3 although it is tacitly assumed that only one mode is excited at each port.

The input-output relations of the "four-port" comparator are described by the matrix equation

$$\mathbf{b} = \mathbf{S}\mathbf{a} \quad (1)$$

where  $\mathbf{a}$  and  $\mathbf{b}$  are column matrices representing incident and scattered waves, respectively, and  $\mathbf{S}$  is the scattering matrix. At ports 3 and 4, incident and scattered waves are related by

$$\rho_r = a_3/b_3 \quad (2)$$

and

$$\rho_x = a_4/b_4, \quad (3)$$

while null output at port 6 yields

$$b_6 = 0. \quad (4)$$

Combining (1) through (4) leads to the linear, homogeneous set

$$\begin{aligned} (S_{33}\rho_r - 1)b_3 + S_{34}\rho_x b_4 + S_{35}a_5 &= 0 \\ S_{34}\rho_r b_3 + (S_{44}\rho_x - 1)b_4 + S_{45}a_5 &= 0 \\ S_{36}\rho_r b_3 + S_{46}\rho_x b_4 + S_{56}a_6 &= 0 \end{aligned} \quad (5)$$

whose solution exists if, and only if, the determinant of the coefficients is zero. Equating this determinant to zero yields an equation of the form

$$\rho_x = \frac{\alpha\rho_r + \delta}{\gamma\rho_r + 1} \quad (6)$$

where  $\alpha$ ,  $\delta$ , and  $\gamma$  are complex constants given by

$$\alpha = \frac{\{S_{36}S_{56} - S_{33}S_{55}\}}{\{S_{44}S_{56} - S_{46}S_{45}\}} \quad (7)$$

$$\delta = \frac{\{S_{56}\}}{\{S_{44}S_{56} - S_{46}S_{45}\}} \quad (8)$$

and

$$\gamma = \frac{\{(S_{34}^2 - S_{33}S_{44})S_{56} + (S_{46}S_{33} - S_{34}S_{35})S_{46} + (S_{44}S_{35} - S_{34}S_{45})S_{36}\}}{S_{44}S_{56} - S_{46}S_{45}} \quad (9)$$

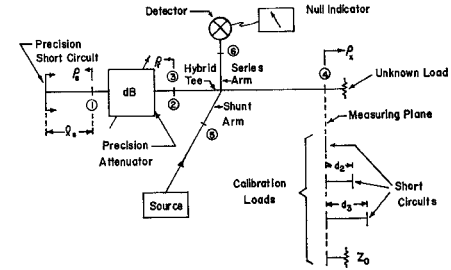


Fig. 1. Schematic diagram of basic reflection coefficient bridge including calibration loads. Although the comparator network is shown to be a hybrid tee, the analysis actually applies to any "four-port" capable of yielding null output at balance.

measurements will be required to determine  $\alpha$ ,  $\delta$ , and  $\gamma$ .

Another fairly significant error that can be greatly reduced by preliminary measurements arises from reflections at the input ports of the rotary-vane attenuator. Such reflections are themselves functions of the attenuator setting. Holm et al. [7], have shown, however, that to a good approximation the attenuator's scattering coefficients are of the form

$$S_{12} = A_{12} \cos^2 \theta$$

$$S_{11} = A_{11} + B_{11} \sin^2 \theta + C_{11} \sin^2(2\theta)$$

$$S_{22} = A_{22} + B_{22} \sin^2 \theta + C_{22} \sin^2(2\theta) \quad (10)$$

where  $\theta$  is the vane angle and is related to the attenuator setting in decibels by

$$\cos^2 \theta = 10^{-dB/20}, \quad (11)$$

and where  $A_{ii}$ ,  $B_{ii}$ , and  $C_{ii}$  are constants. The constant  $A_{12}$  contains the insertion loss of the attenuator. One can show further that  $\rho_r$  is given by

$$\rho_r = \frac{S_{12}^2 \rho_x}{1 - S_{11} \rho_x} + S_{22} \quad (12)$$

where, for a precision short circuit in which a plane of constant phase moves linearly with position,

$$\rho_s = K_s e^{-j\beta_s l_s}. \quad (13)$$

Combining (6) and (10) through (13), while utilizing the experimentally justified [7] approximations

$$\begin{aligned} |S_{11}| &\ll 1 \\ |C_{22}| &\ll |B_{22}|, \end{aligned} \quad (14)$$

and neglecting products of small terms, yields finally an equation of the form

$$\rho_x = \frac{K_1 \{10^{-dB/10} e^{-j2\beta_s l_s}\} + K_2 \{1 - 10^{-dB/20}\} + K_3}{K_4 \{10^{-dB/10} e^{-j2\beta_s l_s}\} + 1} \quad (15)$$

One can show that (6) reduces simply to  $\rho_x = \rho_r$  for the special case of perfect symmetry. In general, however, at least three preliminary

where  $K_1$ ,  $K_2$ ,  $K_3$ , and  $K_4$  are complex constants that describe the overall bridge network. For an "ideal" bridge,  $|K_1|$  would equal unity

Manuscript received July 5, 1966; revised December 15, 1966, and April 10, 1967. This work was supported by the Air Force Office of Scientific Research, Office of Aerospace Research under Grant AF-AFOSR-606-67, and by the National Science Foundation under Grant GK-1272.

while  $K_2$ ,  $K_3$ , and  $K_4$  would be zero.

Calibration of the bridge may be accomplished by performing preliminary balances with known values of  $\rho_x$  and simultaneously solving (15) for  $K_1$  through  $K_4$ . A digital computer has proven an invaluable aid in performing this mathematical step. For the rectangular  $TE_{10}$  mode, we have calibrated the bridge with three short circuits spaced approximately 120 degrees apart (Fig. 1) followed by a matched termination that had been tuned for zero reflections with a tuned reflectometer [2]. This procedure has yielded accuracies better than 0.001 in magnitude and  $\frac{1}{2}$  degree in phase over the entire range  $0 \leq |\rho| \leq 1$  at 10 and 24 GHz.

With the circular  $TE_{01}$  mode, a well-matched termination is difficult to achieve. We have, therefore, extended the technique to include five preliminary balances: three with short circuits; one with a "matched" termination; and one more with the "matched" termination shifted by approximately one-quarter wave. The resultant five equations were then solved simultaneously for  $K_1$ – $K_4$  and also for the reflection coefficient of the "matched" termination. This procedure has yielded accuracies better than 0.01 in magnitude and 1 degree in phase for  $0 \leq |\rho| \leq 1$  at 24, 48, and 70 GHz. We believe that the ultimate accuracy of the circular  $TE_{01}$  mode bridges is presently being limited by the modal purity of the available mode transducers.

Differences in the electrical path lengths of reference and sample arms will cause bridge balance to be frequency sensitive. For maximum phase precision, therefore, one should take steps to insure that these paths are nearly equal and that the frequency of the oscillator is stable. Electronic control [8] of the klystron oscillator frequency has proven to be a desirable refinement.

KEITH S. CHAMPLIN  
JOHN D. HOLM

Dept. of Elec. Engrg.  
University of Minnesota  
Minneapolis, Minn. 55455  
DONALD B. ARMSTRONG<sup>1</sup>  
Electron Tube Div.  
Litton Industries  
San Carlos, Calif.

## REFERENCES

- [1] S. Roberts and A. von Hippel, "A new method for measuring dielectric constant and loss in the range of centimeter waves," *J. Appl. Phys.*, vol. 17, pp. 610–616, July 1946.
- [2] G. F. Engen and R. W. Beatty, "Microwave reflectometer techniques," *IRE Trans. Microwave Theory and Techniques*, vol. MTT-7, pp. 351–355, July 1959.
- [3] A. F. Pomeroy, "Evaluation of uncertainties in measurement of electrical echoes in waveguide lines," *Microwave J.*, vol. 5, pp. 72–77, November 1962.
- [4] H. G. Beljers and W. J. van der Lindt, "Dielectric measurements with two magic tees on shorted waveguides," *Phillips Research Rept.*, vol. 6, pp. 96–104, 1951.
- [5] C. W. van Es, M. Gevers, and F. C. de Ronde, "Waveguide equipment for 2 mm microwaves—II," *Phillips Tech. Rev.*, vol. 22, pp. 181–216, March 1961.
- [6] K. S. Champlin, J. D. Holm, and G. H. Glover, "Electrodeless determination of semiconductor conductivity from  $TE_{00}$ —mode reflectivity," *J. Appl. Phys.*, vol. 38, pp. 96–98 January 1967.

<sup>1</sup> Formerly with the Dept. of Elec. Engrg., University of Minnesota, Minneapolis, Minn.

- [7] J. D. Holm, D. L. Johnson, and K. S. Champlin, "Reflections from rotary-vane precision attenuators," *IEEE Trans. Microwave Theory and Techniques (Correspondence)*, vol. MTT-15, pp. 123–124, February 1967.
- [8] R. V. Pound, "Frequency stabilization of microwave oscillators," *Proc. IRE*, vol. 35, pp. 1405–1415, December 1947.

## Magnetodynamic Modes in Axially Magnetized Ferrite Rods Between Two Parallel Conducting Sheets

Open electromagnetic resonators are well-known structures for many applications in the microwave region [1]. Assuming a lossless nonconducting medium partly surrounded by perfectly conducting metal walls, a manifold of undamped oscillations may exist provided the energy of the corresponding electromagnetic field (with finite amplitude) remains finite. In practice, high  $Q$  modes occur in open resonators built from isotropic or anisotropic dielectrics [2], [9] or ferrites [3], [4] partly enclosed by well conducting metal walls. In the case of ferrites, the resonator is tunable by a dc magnetic field which may be useful for many technical applications.

In this correspondence, the open resonator shown in Fig. 1 will be investigated. One azimuthally symmetric mode of this resonator structure has been described earlier [4]. All nonradiating electromagnetic eigensolutions of  $e^{i\omega t}$  time dependence will be analyzed in the following. The rod is homogeneously magnetized to saturation (saturation magnetization  $M_s$ ) in  $z$  direction by a biasing dc magnetic field  $H_0^i$ . The ferrite is assumed to be lossless; the conductivity of the metal walls shall be perfect. The intensities of the RF electromagnetic fields are supposed to be so small that the linear relation

$$B_f = \mu_0 [\mu_1 H_{if} + j\mu_2 (i_z \times H_{if}) + H_{zf} i_z] \quad (1)$$

between the magnetic induction  $B$  and the magnetic field  $H$  is valid. In (1)

$$\mu_1 = 1 + \frac{h_0^i}{h_0^{i2} - w^2}, \quad \mu_2 = - \frac{w}{h_0^{i2} - w^2}, \quad (2)$$

where

$$h_0^i = \frac{H_0^i}{M_s}, \quad w = \frac{f}{f_m}. \quad (3)$$

Here is

$$f_m = - \frac{\gamma_0}{4\pi} \cdot g \cdot M_s$$

( $g = g$  factor, the free electron gyromagnetic ratio  $\gamma_0 = -2.21 \cdot 10^7$  cm/A·s  $f = \omega/2\pi$  = frequency).

The boundary conditions of the electric field  $E$  and the magnetic induction on the metal sheets can be met by

$$E_{if,a} = F_{if,a} \sin \beta z, \quad (2)$$

$$E_{zf,a} = F_{zf,a} \cos \beta z, \quad (3)$$

$$H_{if,a} = G_{if,a} \cos \beta z, \quad (4)$$

$$H_{zf,a} = G_{zf,a} \sin \beta z, \quad (5)$$

Manuscript received July 5, 1966; revised March 16, 1967. This work was supported by the Deutsche Forschungsgemeinschaft.

where

$$\beta = \frac{\pi}{l} \rho \quad (\rho = 0, 1, 2, \dots). \quad (6)$$

Subscript "f" denotes fields in the ferrite, subscript "a" characterizes fields in the air-filled region. According to Kales [6], differential equations of the  $z$  components (subscript  $z$ ) can be set up from Maxwell's equations. By vector operations, it is possible to derive the transverse components (subscript  $t$ ) from the  $z$  components. The Kales' formulas are modified to

$$F_{zf} = \frac{b}{s_1 - a} u_{1f} + u_{2f}, \quad (7)$$

$$G_{zf} = u_{1f} + \frac{s_2 - a}{b} u_{2f} \quad (8)$$

to get also the solution of an infinitely high dc magnetic field, where the ferrite behaves as an isotropic medium [10]. Here  $s_1$  and  $s_2$  are defined by

$$s_{1,2} = \frac{1}{2} [a + c \mp \sqrt{(a - c)^2 + 4bd}], \quad (9)$$

if  $s_1$  has the minus sign and  $s_2$  the plus sign of the square root, respectively. In (9) are

$$a = g^2 - \frac{\mu_2}{\mu_1} k^2, \quad b = -\omega \mu_0 \beta \frac{\mu_2}{\mu_1},$$

$$c = \frac{g^2}{\mu_1}, \quad d = -\omega \epsilon_0 \epsilon_f \beta \frac{\mu_2}{\mu_1},$$

with

$$g^2 = \frac{\omega^2}{c_0^2} \epsilon_f \mu_1 - \beta^2, \quad k^2 = \frac{\omega^2}{c_0^2} \epsilon_f \mu_2.$$

( $\epsilon_f$  is the relative permittivity of the ferrite material and  $c_0$  the velocity of the light in vacuum.)

The solutions of the differential equations of the  $z$  components in cylindrical coordinates are

$$u_{1f} = A_m Z_m(\sigma_1 r) e^{im\phi}, \quad (10)$$

$$u_{2f} = B_m Z_m(\sigma_2 r) e^{im\phi}, \quad (11)$$

$$G_{za} = C_m K_m(hr) e^{im\phi}, \quad (12)$$

$$F_{za} = D_m K_m(hr) e^{im\phi}, \quad (13)$$

where

$$m = 0, \pm 1, \pm 2, \dots$$

In these equations

$$h^2 = \beta^2 - \frac{\omega^2}{c_0^2}, \quad \sigma_{1,2} = \sqrt{|s_{1,2}|},$$

$$Z_m(\sigma_1,2r) = J_m(\sigma_1,2r) \quad \text{for } s_{1,2} > 0,$$

$$Z_m(\sigma_1,2r) = I_m(\sigma_1,2r) \quad \text{for } s_{1,2} < 0.$$

$J_m$  means the Bessel function of order  $m$ ,  $I_m$  is the modified Bessel function of the first kind and of the order  $m$ ,  $K_m$  is the modified Bessel function of the second kind and of the order  $m$ .

Nonradiating eigensolutions only exist for  $h^2 > 0$ , i.e.,  $z$  independent nonradiating eigensolutions are not possible. The eigenvalue equation is obtained by meeting the continuity conditions at  $r = r_0$

$$A_{11} A_{22} - A_{12} A_{21} = 0. \quad (14a)$$